Model-Based 3D/4D Image Reconstruction: Incorporation of Prior Information

Guang-Hong Chen, PhD

Professor of Medical Physics and Radiology

DEPARTMENTS OF Medical Physics & Radiology
UNIVERSITY OF WISCONSIN SCHOOL OF MEDICINE AND PUBLIC HEALTH

Outline

- Model Based Image Reconstruction: Filtered Backprojection (FBP)
- Model based Image Reconstruction: Statistical Model Based Iterative Reconstruction
- Model Based Imaging Reconstruction: Prior Image Constrained Compressed Sensing (PICCS)
- Model Based Image Reconstruction: Beyond the original PICCS
- Discussion and conclusions

2

Outline

- Model Based Image Reconstruction: Filtered Backprojection (FBP)
- Model based Image Reconstruction: Statistical model based iterative reconstruction (SIR)
- Model Based Imaging Reconstruction: Prior Image Constrained Compressed Sensing (PICCS)
- Model Based Image Reconstruction: Beyond the original PICCS
- Discussion and conclusions

3

Filtered Backprojection (FBP)

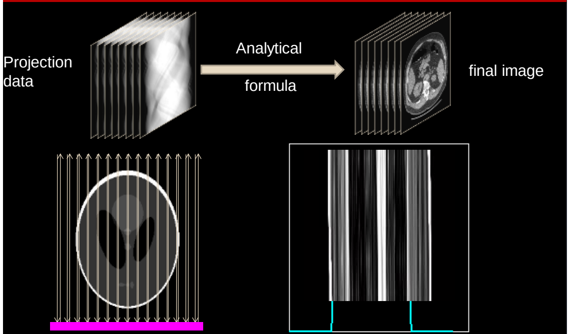

Textbooks by Jiang Hsieh, or by Kak & Slaney

4

A model in FBP Reconstruction?

Beer-Lambert Law: $\bar{I} = \bar{I}_0 e^{-\int_0^d ds\,\mu(\vec{x};E)}$ $\quad \ln\frac{\bar{I}_0}{\bar{I}} = \int_0^d ds\,\mu(\vec{x},E)$

Ensemble Average is needed:

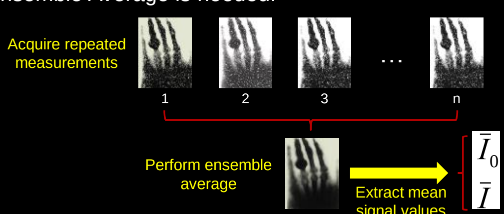

5

A model in FBP Reconstruction

- In FBP Reconstruction: We use one sample to represent the mean, since it is harmful and time-consuming to obtain a true ensemble average.
- Data Model in FBP: Use data as if there are no photon statistical fluctuations in data acquisition!

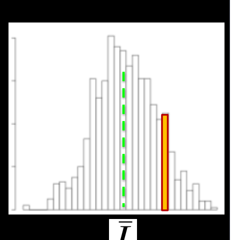

Advice from a wise man

George E. P. Box
(1919-2013)

"Remember that all models are wrong; the practical question is how wrong do they have to be to not be useful."

Box, G. E. P., and Draper, N. R., (1987), *Empirical Model Building and Response Surfaces, John Wiley & Sons, New York,* p. 74

7

How wrong is the model used in FBP?

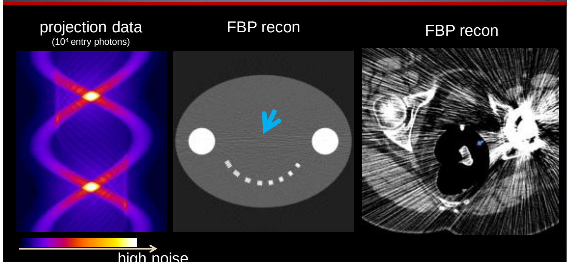

The non-fluctuation model is quite good except for very low exposure/dose levels!

8

Outline

- Model Based Image Reconstruction: Filtered Backprojection (FBP)
- Model based Image Reconstruction: Statistical Image Reconstruction (SIR)
- Model Based Imaging Reconstruction: Prior Image Constrained Compressed Sensing (PICCS)
- Model Based Image Reconstruction: Beyond the original PICCS
- Discussion and conclusions

9

Problem statement

- How should we incorporate the actual photon fluctuations into the CT image reconstruction?
- For simplicity, let's assume a perfect photon counting detector is used (a model again, sorry!).

10

Poisson data model for low exposures

We cannot perform repeated measurements to obtain the experimental mean, but what else do we know about the measurement?

Probability!

$$P(I_k) = e^{-\bar{I}} \frac{\bar{I}^{I_k}}{I_k!}$$

Joint probability of a data set:

$$P(\{I_k\} \mid \mu) = \prod_{k=1}^{M} e^{-\bar{I}_k} \frac{\bar{I}_k^{I_k}}{I_k!}$$

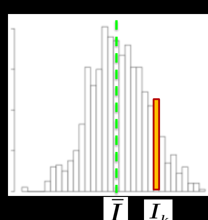

11

Inverse problem

What is the probability to estimate one attenuation distribution of an image object given that the measured data set in your hand?

Bayesian rule $P(\{N_i\} \mid \mu) \propto P(\mu \mid \{N_i\}) = \frac{P(\{N_i\} \mid \mu) P(\mu)}{P(\{N_i\})}$

Image Reconstruction problem statement:

Seek for an estimation to maximize the probability!

12

Maximum Likelihood (ML) method

- Maximizing the Log-likelihood function:

$$\vec{\mu} =: \arg\max_{\mu}[\ln P(\mu(\vec{x},E)\,|\,\{N_i\})] = \arg\max_{\mu}[\sum_{i=1}^{M}(-\bar{N}_i + N_i \ln \bar{N}_i - \ln N_i) + \ln P(\vec{\mu})]$$

- Under the following quadratic approximation:

$$\vec{\mu} = \arg\min_{\mu}[\frac{1}{2}(\vec{y} - A\vec{\mu})^T D(\vec{y} - A\vec{\mu}) + \lambda R(\vec{\mu})]$$

$$D = diag\{N_1, N_2, \cdots, N_M\}$$

13

Data model and forward projection

$$y_k = \ln\frac{\bar{I}_0}{\bar{I}_k}$$

$$\int_0^d ds_k \mu(\vec{x},E) = \int_0^d ds_k \sum_j \mu_j B_j(\vec{x},E) = \sum_j \mu_j \int_0^d ds_k B_j(\vec{x},E) = \sum_j A_{kj}\mu_j = [A\vec{\mu}]_k$$

- Same strategy as in FBP: Acquire a single sample to represent the mean since it is harmful and time-consuming to obtain the experimental mean.
- Refined Data Model in Statistical Model Based Iterative Reconstruction: Statistical fluctuations in data acquisition are considered in data usage!

14

Alternating image update and denoising

$$\vec{\mu} = \arg\min_{\mu}[\frac{1}{2}(\vec{y} - A\vec{\mu})^T D(\vec{y} - A\vec{\mu}) + \lambda R(\vec{\mu})]$$

Data consistency driven image update:

$$\vec{v}_{k+1} = \vec{\mu}_k + PA^T D(\vec{y} - A\vec{\mu}_k)$$

Denoising:

$$\vec{\mu}_{k+1} =: \arg\min_{\mu}\left\{\frac{1}{2}\|\vec{\mu} - \vec{v}_{k+1}\|^2_{P^{-1}} + \lambda R(\vec{\mu})\right\}$$

Combettes and Wijs, Multiscale Model. Simul., Vol. 4: 1168(2005)
Li Y, Niu K, Tang J, Chen G-H. SPIE Medical Imaging Proceedings, 2014. p. 90330U-U-8.

15

Benefits of Statistical Model Based Iterative Image Reconstruction

Reduce streaks caused by low photon count (high noise) projection data and reduced noise level

FBP recon

IR w/ stat

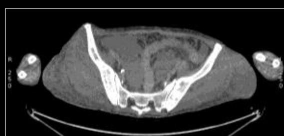

16

Algorithm and Pseudo code: TV Example

Algorithm TV – SIR :

$\boldsymbol{u}^0 \leftarrow u_p,\ \boldsymbol{D}^0 \leftarrow [u_0^{i+1} - u_i, u_0^{i+M} - u_i]^T,\ \boldsymbol{B}^0 \leftarrow \mathbf{0}$

While $||\boldsymbol{A}\mathbf{u}^k - \boldsymbol{f}||_2^2 \geq \varepsilon$ **do**

$\mathbf{v}^{k+1} = \boldsymbol{u}^k + \frac{1}{\delta}\boldsymbol{A}^T\boldsymbol{C}(\boldsymbol{f} - \boldsymbol{A}\boldsymbol{u}^k).$

For $i = 1, 2, ..., MN.$

$u_i^{k+1} = \frac{\delta\mu/\lambda}{\delta\mu/\lambda+4} v_i^{k+1} + \frac{4}{\delta\mu/\lambda+4}(\bar{u}_i^k + h_i^k)$

$\mathbf{d}_i^{k+1} = S_\mu\ (|\boldsymbol{E}_i^{k+1}|)\frac{\boldsymbol{E}_i^{k+1}}{||\boldsymbol{E}_i^{k+1}||_2}$

$\mathbf{b}_i^{k+1} = \boldsymbol{E}_i^{k+1} - \boldsymbol{d}_i^{k+1}.$

End

End

$$
\begin{aligned}
u_i^{k+1} &:= \frac{\delta\mu/\lambda}{\delta\mu/\lambda+4} v_i^{k+1} + \frac{4}{\delta\mu/\lambda+4}(\bar{u}_i^k + h_i^k) \\
\bar{u}_i^k &:= \frac{1}{4}(u_{i+1}^k + u_{i+M}^k + u_{i-1}^k + u_{i-M}^k), \\
h_i^k &:= \frac{1}{4}[(d_{i-1,x}^k - d_{i,x}^k) + (d_{i-M,y}^k - d_{i,y}^k) + (b_{i-1,x}^k - b_{i,x}^k) + (b_{i-M,y}^k - b_{i,y}^k)].
\end{aligned}
$$

Li Y, Niu K, Tang J, Chen G-H. SPIE Medical Imaging Proceedings, 2014. p. 90330U-U-8.

17

Benefit of SIR: Clinical Case

FBP

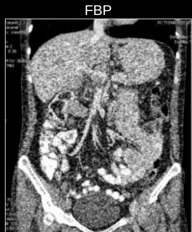

Veo

This Abdomen/Pevis CT scan covers ~40 cm in the *z* direction with a 0.7 mSv effective dose. The BMI of this patient is 19.4.

New Challenges: different 3D Noise Power Spectra

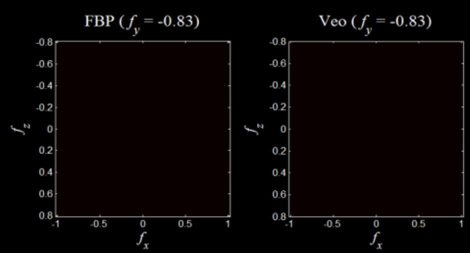

Li, Tang, and Chen, "Statistical Model Based Iterative Reconstruction (MBIR) in clinical CT systems: Experimental assessment of noise performance," *Med. Phys.* (2014)

Joint dependence of spatial resolution on both contrast and radiation dose

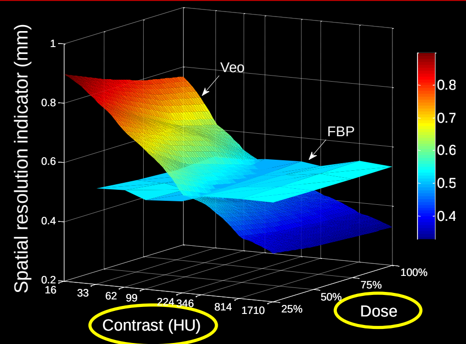

Outline

- Model Based Image Reconstruction: Filtered Backprojection (FBP)
- Model based Image Reconstruction: Statistical Image Reconstruction (SIR)
- Model Based Imaging Reconstruction: Prior Image Constrained Compressed Sensing (PICCS)
- Model Based Image Reconstruction: Beyond the original PICCS
- Discussion and conclusions

21

Problem statement

Besides statistics, if we know a portion of image, or a low spatial resolution representation of an image, or low temporal resolution representation of an image, or even an image with lower energy spectral fidelity, can we incorporate this prior images into reconstruction process?

We define these low resolution images as our prior image.

Prior Image Constrained Compressed Sensing (PICCS)

PICCS $\min[\alpha\|\Psi_1(\mathbf{x}-\mathbf{x}_P)\|_1+(1-\alpha)\|\Psi_2\mathbf{x}\|_1+\frac{\lambda}{2}(\mathbf{Ax}-\mathbf{y})^T D(\mathbf{Ax}-\mathbf{y})]$ *

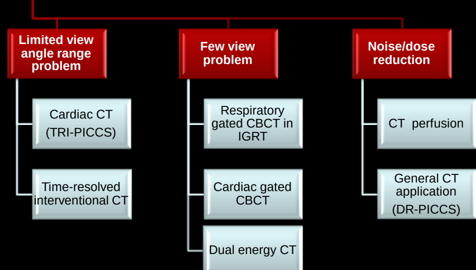

*G.-H. Chen, J. Tang, and S. Leng, Med. Phys. (2008) Vol. 35 p660

PICCS Implementation: Pseudo-Code

Algorithm PICCS – Reconstruction :

$\boldsymbol{u}^0 \leftarrow u_p,\ \boldsymbol{D}^0 \leftarrow [u_0^{i+1}-u_i, u_0^{i+M}-u_i]^T,\ \boldsymbol{B}^0 \leftarrow \mathbf{0}$

While $\|\boldsymbol{A}\mathbf{u}^k-\boldsymbol{f}\|_2^2 \geq \varepsilon$ **do**

  $\mathbf{v}^{k+1}=\boldsymbol{u}^k+\frac{1}{\delta}\boldsymbol{A}^T\boldsymbol{C}(\boldsymbol{f}-\boldsymbol{A}\boldsymbol{u}^k).$

  For $i=1,2,\dots,MN.$

  $u_i^{k+1}=u_i^{k+1}=\frac{\delta\mu/\lambda}{\delta\mu/\lambda+8}\mathbf{v}_i^{k+1}+\frac{4}{\delta\mu/\lambda+8}(2\bar{u}_i^k+u_{p,i}-\bar{u}_{p,i}+h_i^k+h_{p,i}^k)$

  $d_{i,p}^{k+1}=S_{\mu\alpha}\left(|\boldsymbol{E}_{i,p}^{k+1}|\right)\frac{\boldsymbol{E}_{i,p}^{k+1}}{\|\boldsymbol{E}_{i,p}^{k+1}\|}$

  $d_i^{k+1}=S_{\mu(1-\alpha)}\left(|\boldsymbol{E}_i^{k+1}|\right)\frac{\boldsymbol{E}_i^{k+1}}{\|\boldsymbol{E}_i^{k+1}\|}$

  $b_{i,p}^{k+1}=d_{i,p}^{k+1}-E_{i,p}^{k+1}.$

  $b_i^{k+1}=d_i^{k+1}-E_i^{k+1}.$

  End

End

Computational challenge in IR

- Projection data: M (~10^8) (1000x1000x64)
- Image data: N (~10^8) (512x512x400)
- Transform between projection and image domains: M×N
- A full iterative reconstruction method solves a problem of the size of M×N!
  (Due to sparsity the actual size is ~10^{11})
- Computation time is long without additional innovation/reformulation (Veo takes ~ 1 hour for a typical image volume of 300-400 slices)

25

Make recon faster: GPU acceleration

- PICCS has special mathematical structures which enable numerical implementations that enjoy both:
  - fast convergence speed
  - and high parallelizability.
- General purpose graphic cards are used to accelerate the algorithm:
  - Clinical CT volumes can be reconstructed within 1~2 minutes

NVIDIA
CUDA

Optimal choice of the PICCS weighting parameter

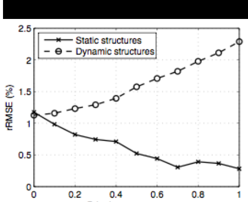

PICCS parameters α & λ: Accuracy

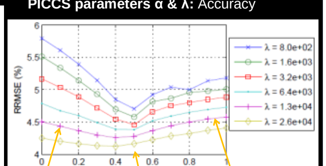

Small α = overly smooth

Large α = visible prior

Optimum: α in [0.4, 0.5]

Observations:
At larger λ, the RRMSE improves (noise level conformity) and the variation between different α decreases.

Thèriault-Lauzier, Tang, and Chen, Med. Phys., (2011)

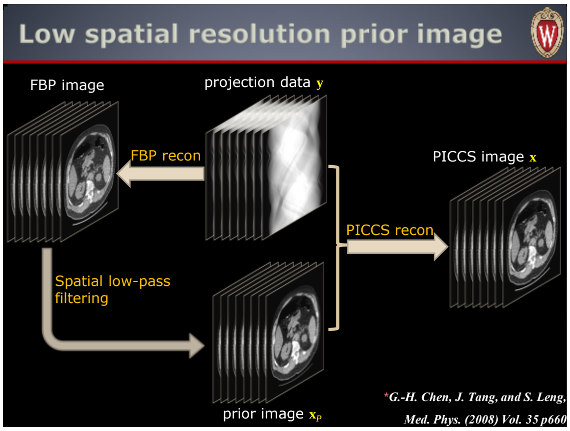
Low spatial resolution prior image
FBP image
projection data y
FBP recon
PICCS image x
PICCS recon
Spatial low-pass filtering
prior image x_p
*G.-H. Chen, J. Tang, and S. Leng, Med. Phys. (2008) Vol. 35 p660

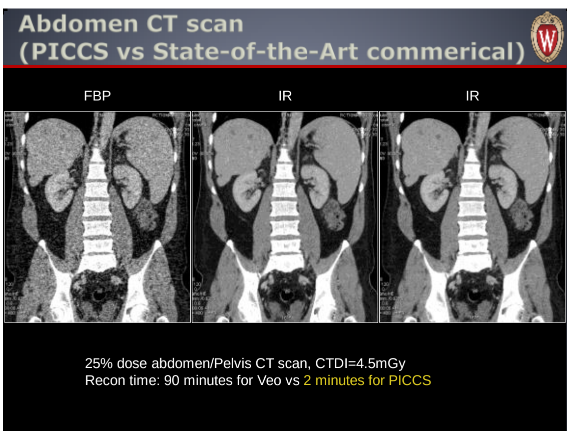
Abdomen CT scan
(PICCS vs State-of-the-Art commerical)
FBP
IR
IR
25% dose abdomen/Pelvis CT scan, CTDI=4.5mGy
Recon time: 90 minutes for Veo vs 2 minutes for PICCS

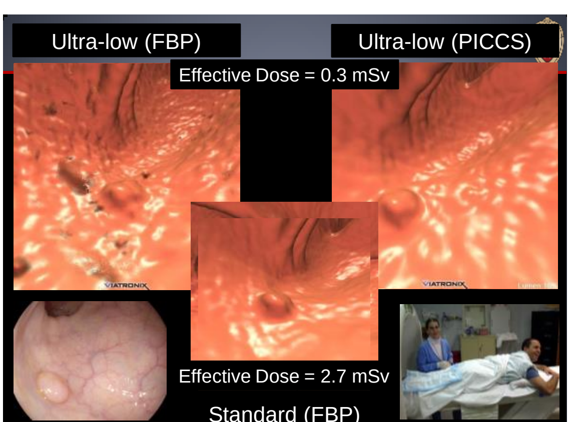
Ultra-low (FBP)
Ultra-low (PICCS)
Effective Dose = 0.3 mSv
Effective Dose = 2.7 mSv
Standard (FBP)

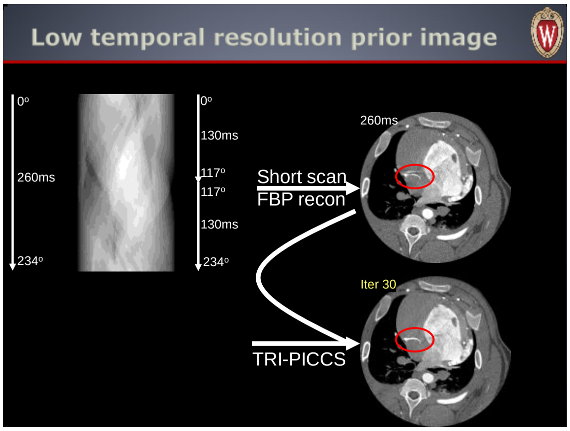
Low temporal resolution prior image
0º
260ms
234º
0º
130ms
117º
117º
130ms
234º
Short scan
FBP recon
260ms
Iter 30
TRI-PICCS

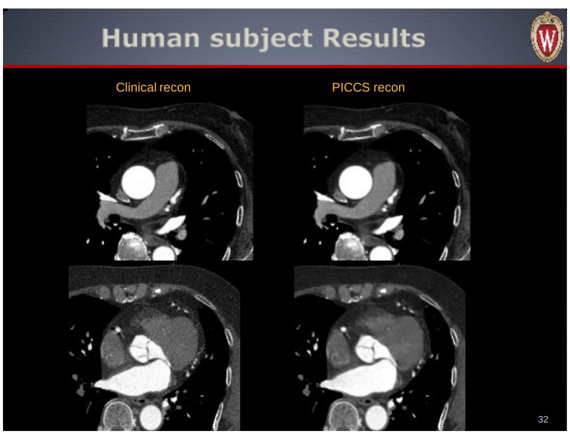
Human subject Results
Clinical recon
PICCS recon
32

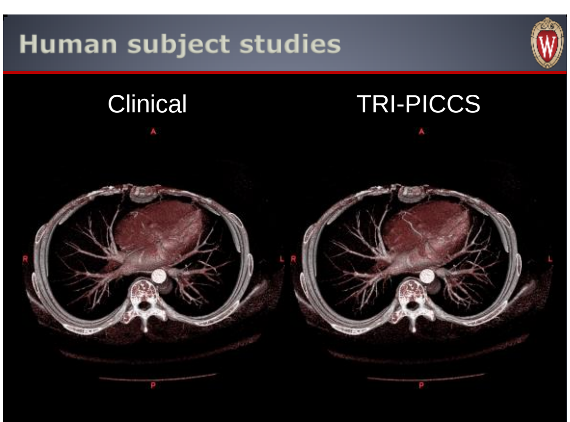
Human subject studies
Clinical
TRI-PICCS

4DCBCT: concept and technical challenge

- Projection data are retrospectively sorted into several phase bins, followed by the reconstruction of each phase bin.

- Undersampled projection data within each phase bin lead to streak artifacts in the reconstructed images when the conventional FBP algorithm is used as in current commercial systems.

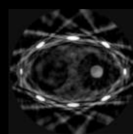

34

PICCS-4DCBCT using a low temporal resolution prior image

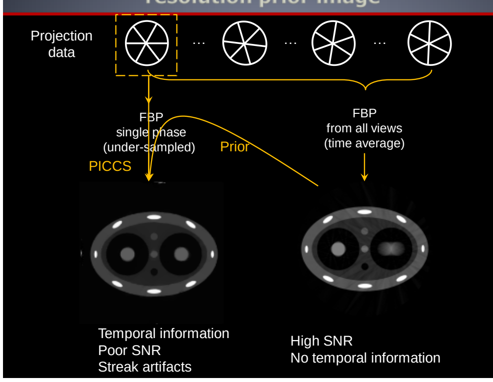

Human subject study

FBP PICCS

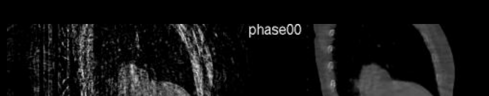

- 1-minute CBCT scan
- RPM based gating
- Large tumor on top of the diaphragm
- Predominant tumor motion in the SI direction

36

Low spectral resolution prior image

- Mixed kV data are collected during the acquisition.
- All of the data are used to reconstruct a mixed kVp image with FBP.
- The undersampled 80 and 140 kV data are fed into the PICCS algorithm with the mixed FBP image as a prior image to reconstruct streak free 80 and 140 kV images.

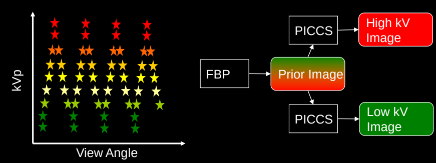

Szczykutowicz and Chen, Phys. Med. Biol. , Vol. 55:6411-6429(2010)

DE-PICCS: Attenuation Images

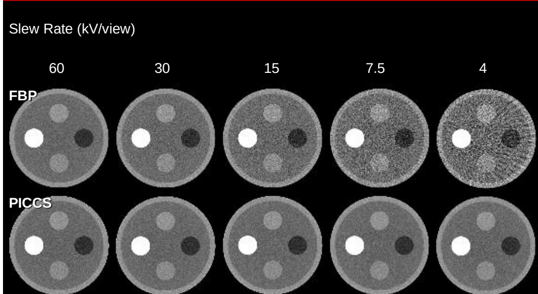

Szczykutowicz and Chen, Phys. Med. Biol. , Vol. 55:6411-6429(2010)

Outline

- Model Based Image Reconstruction: Filtered Backprojection (FBP)
- Model based Image Reconstruction: Statistical Image Reconstruction (SIR)
- Model Based Imaging Reconstruction: Prior Image Constrained Compressed Sensing (PICCS)
- Model Based Image Reconstruction: Beyond the original PICCS
- Discussion and conclusions

39

Norm dependence of PICCS

- Prior Image Constrained Compressed Sensing (PICCS)[1,2]

$$\hat{\mathbf{x}} = \arg\min\left\{\underbrace{\boxed{\frac{/}{2}(A\mathbf{x} - y)^T D(A\mathbf{x} - y)}}_{\text{Data Consistency}} + \underbrace{\boxed{f_{piccs}(\mathbf{x})}}_{\text{PICCS}}\right\}$$

$$f_{piccs}(\mathbf{x}) = a\underbrace{\boxed{\| y(\mathbf{x} - x_p)\|_1}}_{\text{Prior image term}} + (1 - a)\underbrace{\boxed{\| y(\mathbf{x})\|_1}}_{\text{Compressed Sensing term}}$$

From 1-norm to P-norm

$$f_{nd-piccs}(\mathbf{x}) = a\| y(\mathbf{x} - x_p)\|\boxed{{}_p^p} + (1 - a)\| y(\mathbf{x})\|\boxed{{}_p^p} \qquad \alpha \in [0,1] \qquad p \in [1,2]$$

1. Chen et al. Medical Physics 2008
2. PT Lauzier and G-.H Chen. Medical Physics 39(10) 2012

Norm dependence in PICCS

- When the selected norm is higher than 1, it has been suggested that a reweighted scheme may be applied to approximate the result achieved with the L1-norm.
- Thus, an iterative reweighted technique is also applied to study the norm dependence of the performance of PICCS.

1. Gorodnitsky and Rao, IEEE Tran. Signal Processing, Vol.45:600 (1997)
2. Jung, Ye, and Kim, Phys. Med. Biol., Vol. 52:3201(2007)
3. Candes, Wakin, and Boyd, J. Fourier Anal. Applications, Vol.14:877(2008)

41

Reweighted p-norm PICCS

Question to be addressed:

can we replace the 1-norm by a reweighted p-norm in PICCS?

k[th] iteration : $\displaystyle \underset{i}{\text{å}} \frac{f^p}{f_{k-1}^{p-1}} = \| f \|_1^1$

Li, Tang, and Chen, Proc. SPIE 8668: 86681M (2013)

42

RMSE vs. view number & p-norm

W/O REWEIGHTED SCHEME | **W/ REWEIGHTED SCHEME**

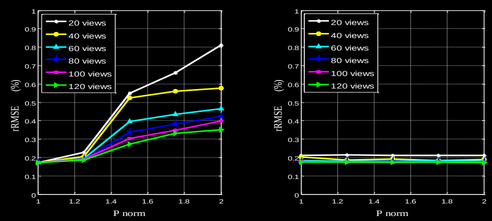

The dependence of reconstruction accuracy on view number and p-norm is decoupled with the reweighted scheme

Li, Tang, and Chen, Proc. SPIE 9033:903308 (2014)

43

Non-convex PICCS (NC-PICCS)

- In the NC-PICCS framework, the $\mathcal{L}_1$ norm is replaced with a non-convex norm ($\mathcal{L}_p$ with p<1)
- This may be used for both PICCS as well as conventional CS
- NC-PICCS provides high quality images with minimal artifacts, even in cases with very few view angles

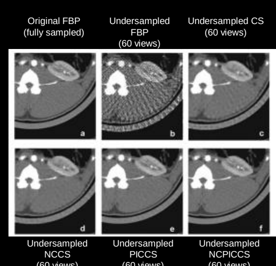

Ramirez-Giraldo, *et al.*, *Nonconvex prior image constrained compressed sensing (NCPICCS): Theory and simulations on perfusion CT, Med. Phys. Vol. 38, No. 4, pp2157 (2011).*

44

Adaptive Prior Image Constrained Compressed Sensing (APICCS)

- In the APICCS framework, image registration and a weighted relaxation map are used
- This helps ensure good correspondence between the prior image and the reconstructed image
- This is valuable in CBCT for image guided radiation therapy and other applications where a perfectly co-registered prior image may not be available

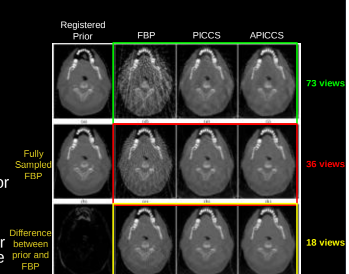

Nett et al, Proc. SPIE 72582: 725803 (2009)

Lee, *et al.* (2012), *Improved compressed sensing-based one-beam CT reconstruction using adaptive prior image constraints, Phys. Med. and Biol. Vol. 57, pp2287.*

45

Deformable Prior Images in Model-based Reconstruction

Initial Imaging Study

Time Passes Between Studies

Motion, Deformation, Anatomical Change

Follow-up Imaging Study

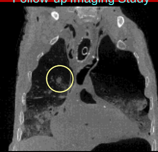

dPIRPLE: (deformable) Prior Image Registration Penalized Likelihood Estimation:

$$\left\{\hat{\mu},\hat{\lambda}\right\} = \arg\max_{\mu} \log L\left(y;\mu\right) - \beta_R \left\|\mathbf{\Psi}_R \mu\right\| - \beta_P \left\|\mathbf{\Psi}_P\left(\mu - \mathbf{W}(\lambda)\mu_P\right)\right\|$$

Statistical Data Fit Term

Traditional Roughness Penalty Term

Prior Image (deformable) Registration Penalty Term

Jointly solve for the image volume (μ) and the deformable registration parameters (λ) within a statistical reconstruction framework and using sparsity-enforcing penalties

H. Dang, A. Wang, Z. Zhao, M. Sussman, J. H. Siewerdsen, and J. W. Stayman, "Joint estimation of deformation and penalized-likelihood CT reconstruction using previously acquired images," *Int'l Mtg. Fully 3D Image Recon. in Radiology and Nuc. Med.*, Lake Tahoe, June 16-21, 2013.

dPIRPLE, Lung Nodule Surveillance

Reconstructions of a Follow-up scan acquisition:

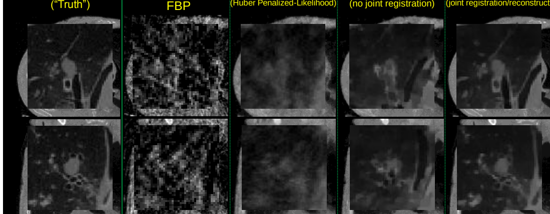

H. Dang, A. Wang, M. S. Sussman, J. H. Siewerdsen, J. W. Stayman, "dPIRPLE: A joint estimation framework for deformable registration and penalized-likelihood CT image reconstruction using prior images," *Physics in Medicine and Biology*, in press.

Discussion and conclusions

- Introduction of statistical model enables improved CT image reconstruction at low photon counts scenarios;
- Introduction of low resolution prior images together with statistical models help further improve CT image reconstruction in a few clinical scenarios;
- Image quality assessment should be performed with care, it is highly recommended to have imaging task in mind for quality assessment.

48

Model-Based Image Reconstruction

"Essentially, all models are wrong; but some are useful."

Box, G. E. P., and Draper, N. R., (1987), *Empirical Model Building and Response Surfaces, John Wiley & Sons, New York,* p. 424

49

Acknowledgements

Medical Physics: Jie Tang, Shuai Leng, Brian Nett, Zhihua Qi, Pascal Thèriault-Lauzier, Tim Szczykutowicz, Steve Brunner, Ke Li, Kai Niu, Yinsheng Li, John Garrett, Nick Bevins, Joe Zambelli, and Ranjini Tolokanahali.

Radiology Department: Perry Pickhardt, Meg Lubner, David Kim, Chris Francois, Jeff Kanne, Cris Myer, Mark Schiebler, Tom Grist, Howard Rowley, Pat Turski, Charlie Strother, and Bev Kienietz

Human Oncology: Minesh Mehta, George Cannon, Mark Ritter, Lauren Shapiro, Jeni Smilowitz, Bhudatt Pawliwal, and John Bayouth

Thank You

Computational challenge in IR

- Projection data: M (~10^8) (1000x1000x64)
- Image data: N (~10^8) (512x512x400)
- Transform between projection and image domains: M×N
- A full iterative reconstruction method solves a problem of the size of M×N!
  (Due to sparsity the actual size is ~10^{11})
- Computation time is long without additional innovation/reformulation (Veo takes a few hours for a typical image volume of 300-400 slices)

52

Make recon faster: GPU acceleration

- PICCS has special mathematical structures which enable numerical implementations that enjoy both:
  - fast convergence speed
  - and high parallelizability.
- General purpose graphic cards are used to accelerate the algorithm:
  - Clinical CT volumes can be reconstructed within 1~2 minutes

PICCS Implementation: more familiar unconstrained optimization method

Idea: reformulate the constraint into a penalty term

$$f_{uc} = \frac{f_{piccs}(\mathbf{x})}{|\psi(\mathbf{x_p})|_{\ell_1}} + \frac{\lambda}{2}\frac{\|\mathbf{Ax} - \mathbf{y}\|^2}{\|\mathbf{Ax_p}\|^2}.$$

$$\arg\min_{x} \; f_{uc}.$$

Data consistency term

α: PICCS parameter a.k.a prior image parameter
λ: data consistency parameter

Thèriault-Lauzier, Tang, and Chen, Med. Phys., (2011)

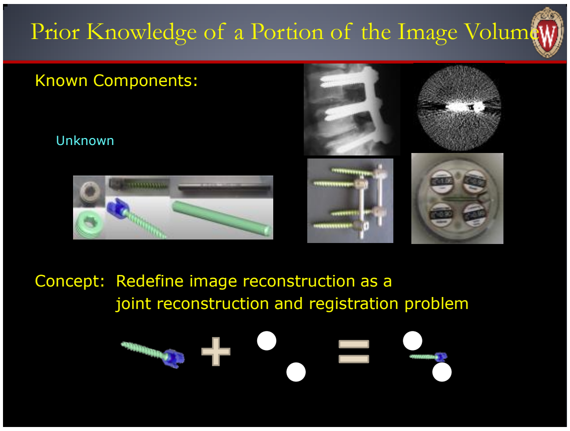
Prior Knowledge of a Portion of the Image Volume
Known Components:
Unknown
Concept: Redefine image reconstruction as a
joint reconstruction and registration problem
+
=

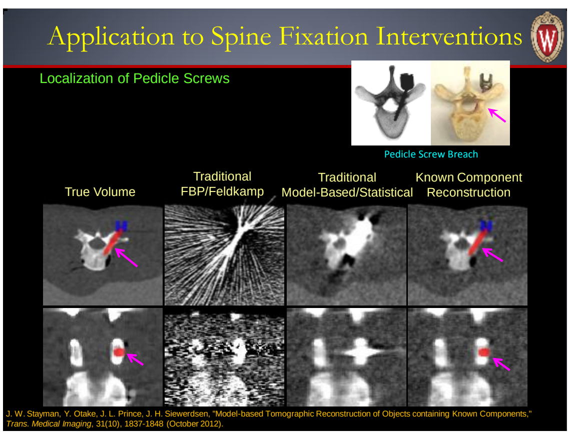
Application to Spine Fixation Interventions
Localization of Pedicle Screws
Pedicle Screw Breach
True Volume
Traditional FBP/Feldkamp
Traditional Model-Based/Statistical
Known Component Reconstruction
J. W. Stayman, Y. Otake, J. L. Prince, J. H. Siewerdsen, "Model-based Tomographic Reconstruction of Objects containing Known Components," Trans. Medical Imaging, 31(10), 1837-1848 (October 2012).

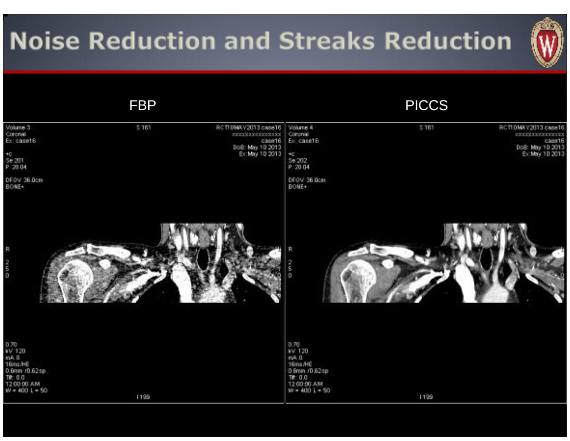
Noise Reduction and Streaks Reduction
FBP
PICCS

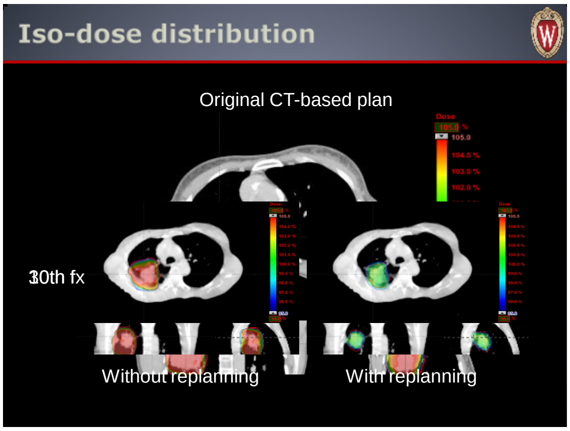
Iso-dose distribution
Original CT-based plan
30th fx
Without replanning
With replanning

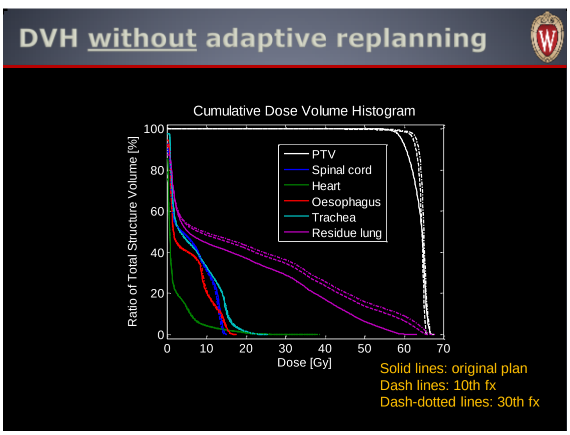
DVH without adaptive replanning
Cumulative Dose Volume Histogram
Ratio of Total Structure Volume [%]
Dose [Gy]
PTV
Spinal cord
Heart
Oesophagus
Trachea
Residue lung
Solid lines: original plan
Dash lines: 10th fx
Dash-dotted lines: 30th fx

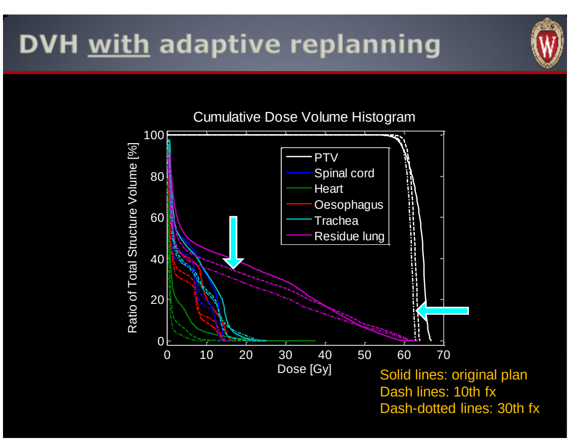
DVH with adaptive replanning
Cumulative Dose Volume Histogram
Ratio of Total Structure Volume [%]
Dose [Gy]
PTV
Spinal cord
Heart
Oesophagus
Trachea
Residue lung
Solid lines: original plan
Dash lines: 10th fx
Dash-dotted lines: 30th fx

Dose statistics comparison

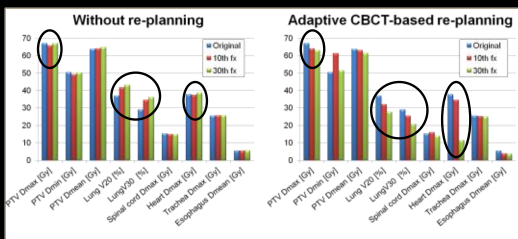

Image Slide Show: Cardiac CT

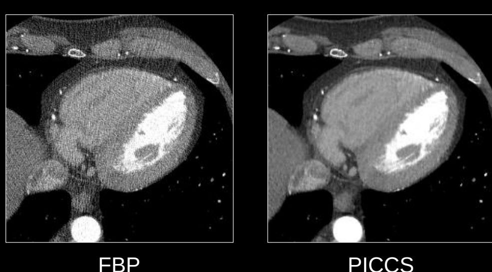

HD750, 100 kVp, 800mA, 0.35s
0.625 mm slice thickness, W/L=700/100 HU

67

Chest CT

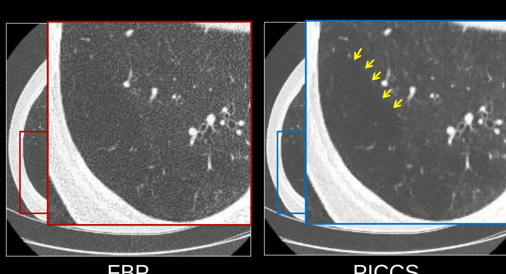

HD750, 120 kVp, $CTDI_{vol}$=0.8 mGy (1/4 SOC dose)
1.25 mm slice thickness, bone+, W/L=1500/-700 HU

68

PICCS on GE Discovery CT750 HD

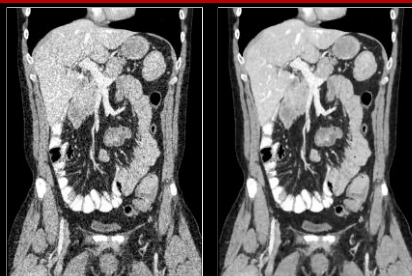

FBP PICCS

120 kVp, $CTDI_{vol}$ 5 mGy.
coronal reslice, $0.66x0.66x0.66\ mm^3$, W/L=324/15 HU

69

PICCS on Siemens SOMATOM Definition Flash

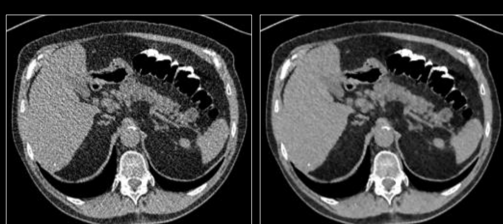

FBP PICCS

1 mm slice thickness, W/L=324/15 HU

70

PICCS on Siemens SOMATOM Definition Flash

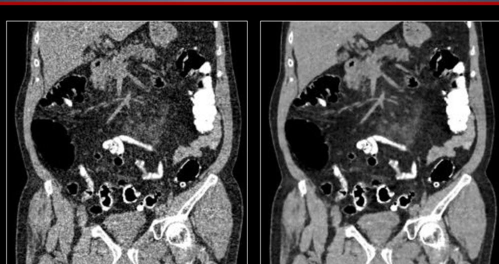

FBP PICCS

coronal reslice, $0.78x0.78x0.78\ mm^3$, W/L=324/15 HU

71

PICCS on Toshiba Aquilion ONE

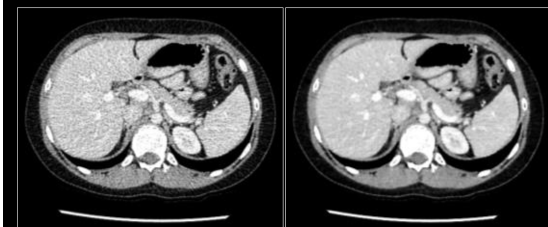

FBP PICCS

0.5 mm slice thickness, W/L=330/35 HU

72

PICCS on Toshiba Aquilion ONE

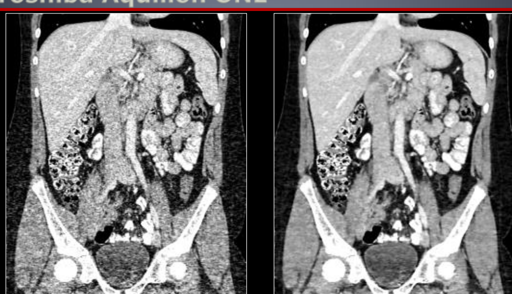

FBP PICCS

coronal reslice, 0.625x0.625x0.625 mm^3, W/L=330/35 HU

73

Retrospective study design

- 20 human subjects CT colonoscopy cases
- Six 100 mm^2 ROIs were measured for each case
  - 2 from air (inside colon)
  - 2 from fat
  - 1 from kidney
  - 1 from liver

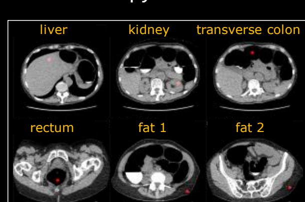

- Images have been read by radiologists who confirmed there were no small structure losses *

* *M. Lubner, P. Pickhardt, J. Tang and G.-H. Chen, Radiology. (2011) Vol. 260 p248*

Mean (CT#)

Mean Attenuation Values of FBP vs. DR-PICCS

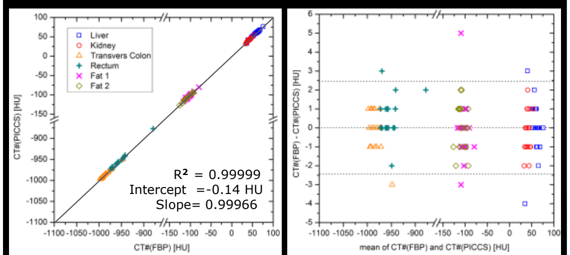

M. Lubner, P. Pickhardt, J. Tang and G.-H. Chen, Radiology. (2011) Vol. 260 p248

Standard Deviation (noise)

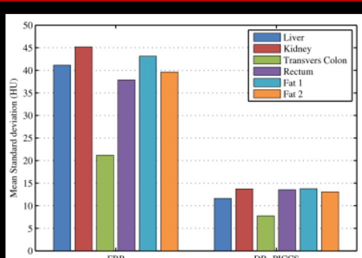

The mean standard deviation is calculated for each ROI over 20 subjects

	Liver	Kidney	Transverse colon	Rectum	Fat 1	Fat 2
Mean NR	3.48	3.21	2.73	2.83	3.06	3.03

Average noise reduction = 3.1

M. Lubner, P. Pickhardt, J. Tang and G.-H. Chen, Radiology. (2011) Vol. 260 p248

Outline

- Iterative reconstruction (IR) methods
- PICCS, a UW-brand IR method, for low dose CT
- Prospective low dose: clinical evaluation
- Challenges and perspectives

77

Prospective low dose study

- Common limitations in most current low dose results:
  - Lack of solid diagnostic value evaluation
  - Retrospective study with low dose methods applied on normal dose scans
  - Lack of truth in low dose scans
  - Very limited number of low dose scans
- A prospective low dose clinical trial with normal dose scan as reference and sufficient number of subjects is needed to validate how low dose techniques should be utilized to benefit clinical diagnosis.

78

Study design – scan and recon

- A low-dose CT series was acquired immediately following the routine standard-dose CT series (HIPAA-compliant, IRB approved protocol)
- Targeted dose reduction 70%-90%
- Ultimate goal 500 subjects
  Initial results included 45 subjects
- Low-dose scans were reconstructed using FBP, ASiR(40%), Veo, PICCS – for evaluation
- Standard-dose scans were reconstructed using FBP – as reference

P. Pickhardt, M. Lubner, D. Kim, J. Tang, R. Julie, A. Munoz del Rio and G. Chen., AJR. (2012) Vol. 199

Study design – results analysis

- Image reformat
  - Reconstructed images were reformatted into 2.5 mm thickness axial and coronal series for review
- Quantitative measurements (four 250 mm^2 ROIs)
  - liver, kidney, muscle, and fat
- Clinical evaluation
  - All images were de-identified and randomized with respect to patients and reconstruction methods.
  - Two expert radiologists reviewed all low-dose series first, then reviewed standard-dose series to serve as clinical reference standard.
  - The results were pooled together from both readers.

Mean (CT#): Bland-Altman plots

Bland-Altman analysis on low-dose scans

	Bias (HU)	Limits (HU)
ASiR	0	0.8
PICCS	0	2.6
Veo	4.3	8.5

ACR QC: CT#(water) = 0±7 HU
Uniformity within ±5 HU

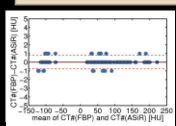
ASiR

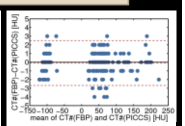
PICCS

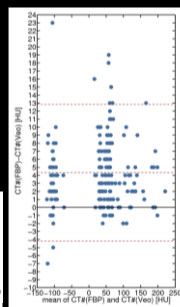
Veo

81

Noise measurements

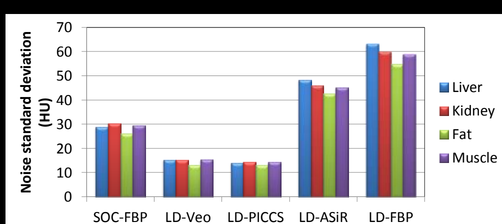

	Veo	PICCS	ASiR
Mean noise reduction	4.0	4.2	1.3

82

Qualitative image quality score criteria: 5-point scale

- 0: non-diagnostic
- 1: severe artifact with low confidence
- 2: moderate artifact or moderate diagnostic confidence
- 3: mild artifact or high confidence
- 4: well depicted without artifacts

Subjective image quality scores

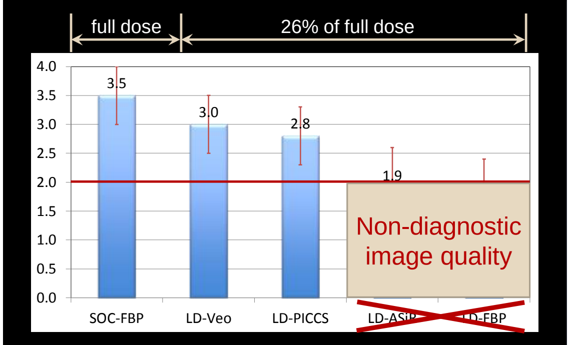

Lesion detection tasks:

- Low contrast lesion detection:
  - Soft-tissue window: W/L=400/50 HU
  - Non-calcific detectable organ-based foci >3 mm
- High contrast stone detection:
  - Bone window: W/L=1200/350 HU
  - Stones >2 mm

Low contrast lesion detection performance

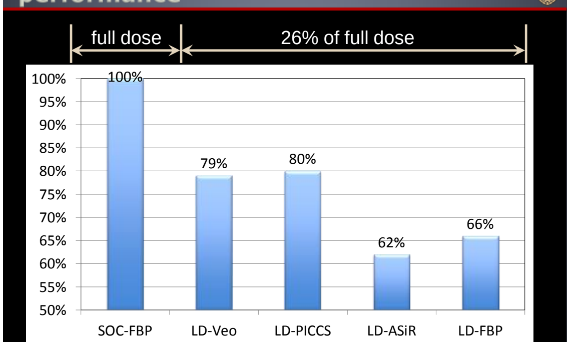

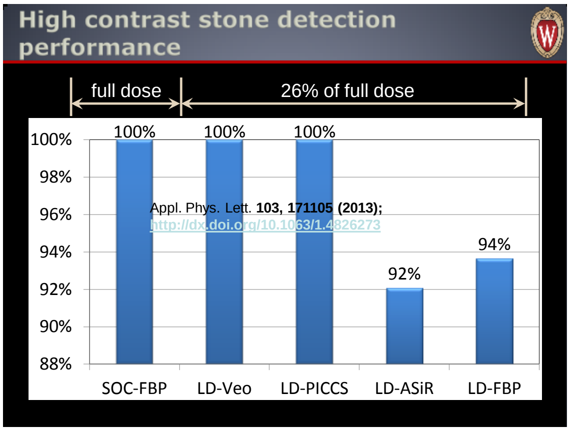
High contrast stone detection performance
full dose
26% of full dose
100%
98%
96%
94%
92%
90%
88%
100%
100%
100%
92%
94%
SOC-FBP
LD-Veo
LD-PICCS
LD-ASiR
LD-FBP
Appl. Phys. Lett. 103, 171105 (2013);
http://dx.doi.org/10.1063/1.4826273